

UC Santa Barbara

UC Santa Barbara Previously Published Works

Title

Integrated optical payload envelope detection and label recovery device for optical packet switching networks

Permalink

<https://escholarship.org/uc/item/1dj3q23c>

Journal

Optics Express, 14(12)

ISSN

1094-4087

Authors

Koch, B R
Hu, Z Y
Bowers, J E
[et al.](#)

Publication Date

2006-06-01

Peer reviewed

Integrated Optical Payload Envelope Detection and Label Recovery Device for Optical Packet Switching Networks

Brian R. Koch, Zhaoyang Hu, John E. Bowers, Daniel J. Blumenthal

Electrical and Computer Engineering Department, University of California, Santa Barbara, California, 93106
koch@ece.ucsb.edu

Abstract: We demonstrate an integrated device for optical payload envelope detection and optical label recovery for optical packet switching. The device is designed to handle asynchronous serially labeled packets with variable length 40 Gbps payloads preceded by 10 Gbps labels. The device outputs two signals: 1. a payload envelope signal corresponding to the temporal location and duration of the optical payload and 2. an electrical label recovered from the optical label. The payload envelope signal has rise and fall times of 3 ns with 150 ps RMS jitter and is used to perform error free label erasure and rewriting. Error free label recovery is also demonstrated.

©2006 Optical Society of America

OCIS codes: 250.3140 Integrated optoelectronic circuits, 060.2360 Fiber optics links and subsystems

References and Links

1. D.J. Blumenthal, B. E. Olsson, G. Rossi, T. E. Dimmick, L. Rau, M. Masonovic, O. Lavrova, R. Doshi, O. Jerphagnon, J. E. Bowers, V. Kaman, L. A. Coldren, and J. Barton, "All-optical label swapping networks and technologies," *IEEE J. Lightw. Technol.*, **18**, 2058-2075 (2000).
2. A. Viswanathan, N. Feldman, Z. Wang, and R. Callon, "Evolution of multiprotocol label switching," *IEEE Commun. Mag.*, **36**, 165-173 (1998).
3. P. Ohlen, B. E. Olsson, and D. J. Blumenthal, "All-optical header erasure and penalty-free rewriting in a fiber-based high-speed wavelength converter," *IEEE Photon. Technol. Lett.*, **12**, 663-665 (2000).
4. Z. Hu, R. Doshi, H. Chou, H. N. Poulsen, D. Wolfson, J. E. Bowers, D. J. Blumenthal, "Optical label swapping using payload envelope detection circuits", *IEEE Photon. Technol. Lett.*, **17**, 1537-1539 (2005).
5. Z. Hu; K. Nishimura; H.F. Chou; L. Rau; M. Usami; J.E. Bowers; D.J. Blumenthal, "40-Gb/s optical packet clock recovery with simultaneous reshaping using a traveling-wave electroabsorption modulator-based ring oscillator", *IEEE Photon. Technol. Lett.*, **16**, 2640-2642 (2004).

1. Introduction

Optical packet switching allows optical networks to scale to a large number of nodes by using optical label swapping [1, 2]. Optical label swapping requires that the label and payload are distinguished from each other in the optical domain. Thus the label can be looked up and erased, and a new label assigned to the same payload without OEO conversion of the payload. In this paper the label is modulated serially before the payload and at a lower bit rate and different modulation format than the payload [3]. Thus only low speed OEO conversion and label processing are required at nodes, and no a-priori knowledge of the incoming packet wavelength or location is required. In this labeling scheme, it is necessary to recover the precise temporal location of the asynchronous variable length payload in order to erase the original labels and subsequently rewrite the new labels. These requirements can be met by using a payload envelope detection (PED) circuit based on optical clock recovery [4]. Another essential task in optical label swapping is label reading in order to route the payloads and determine new labels. This first requires that the optical label gets converted to an electrical signal to be sent to an electronic routing table. A burst mode receiver can perform this task, which we call optical label recovery (OLR). It is desirable to implement the two

tasks of “PED” and “OLR” on the same integrated platform for size, cost, and power reduction. This also demonstrates the potential for integration with even more components.

In this paper we demonstrate a hybrid integrated optoelectronic device to simultaneously achieve PED and OLR for asynchronous optical packets consisting of 40 Gbps return to zero (RZ) variable length payloads and 128 bit 10 Gbps non return to zero (NRZ) labels. The output of the device is an electrical PED signal representing the temporal location of the payload and an electrical label generated by an integrated burst mode receiver. These outputs are intended to be used by an electronic routing table which could use the provided information to perform all tasks required for label erasure, payload routing, and label rewriting, as shown in Figure 1.

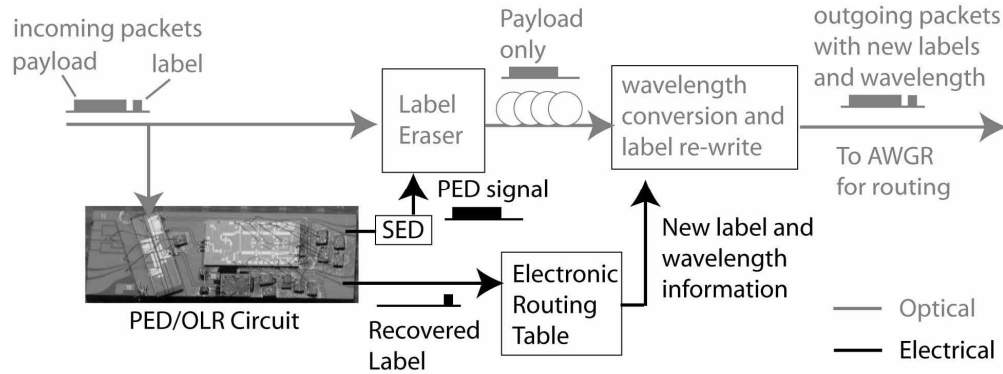


Fig. 1. Integrated PED/OLR device in an optical label swapping network node based on routing by wavelength conversion. SED stands for Schottky envelope detector. AWGR stands for arrayed wavelength grating router.

2. Photonic Device Design

2.1 Device Design and Fabrication

The device consists of a traveling wave photodetector (TWPD) with two RF ports, a semiconductor optical amplifier (SOA), and a photodetector (PD) located serially on the same optical waveguide as shown in Figure 2. The TWPD can also work as a traveling wave electroabsorption modulator (TWEAM) such as reported in other papers to generate recovered optical clocks [4, 5]. The device was fabricated on InP with a semi-insulating substrate. The material has two sets of InGaAsP quantum wells. The TWPD and PD have shallow centered quantum wells for faster response, while the SOA has additional offset quantum wells that provide more gain. The TWPD is 400 μm long, the SOA is 600 μm long, and the PD is 150 μm long after optimizing design. Both the TWPD and the PD have traveling wave electrodes. Bisbenzocyclobutene (BCB) dielectric was used to match the impedance of the electrical coplanar waveguide (CPW) to that of the optical waveguide (about 20 ohms), which allows for higher frequency response. At the edge of the chip, the impedance of the CPW lines is designed to be 50 ohms to match the carrier CPW lines. To minimize reflections, the CPW lines are tapered linearly from the region over the optical waveguide to the edge of the chip.

2.2 Chip on Carrier Implementation

After fabrication the InP device was bonded to an aluminum nitride (AlN) carrier along with electronic devices, as shown in Figure 2. The TWPD and the PD on the InP device were interconnected with the electronic devices on the carrier with the CPW lines and bonded ribbons. For the first task of payload envelope detection, an optoelectronic injection locked loop on the carrier is formed to generate a 40 Gbps packet clock. When a packet enters the TWPD, a photocurrent is generated. This photocurrent is then carried along the CPW lines to a narrowband 36-43 GHz electrical MMIC amplifier on the carrier with 26 dB gain (Mimix Broadband Co., XP1005). The output of this amplifier travels to a CPW based power divider,

which couples out some of the electrical signal as an output. The part remaining in the loop passes through a CPW based Q filter that uses a capacitively coupled resonant section in the inner conductor. A Q factor of 50 was chosen for fast locking time while still maintaining relatively low jitter. The signal coming out of the Q filter returns to the TWPD, combines in phase with the new photocurrent being generated and passes around the loop again. All CPW components have 50 ohm impedance to minimize reflections from external components. When the input optical signal contains a clock frequency within the locking range of the loop, the loop is injection locked through the photocurrent generated in the TWPD. The phase of the loop can be tuned by adjusting the reverse bias voltage of the TWPD or by tuning the gain of the MMIC amplifier.

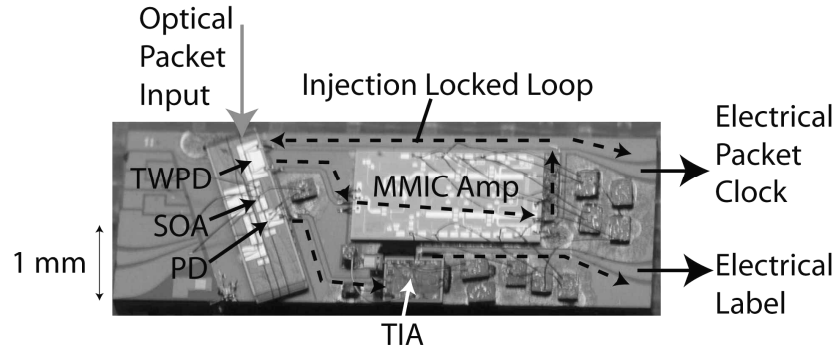


Fig. 2. PED/OLR hybrid integrated device.

With the proper bias voltage on the TWPD, light passes through and then enters the SOA for amplification and then continues to the PD for label recovery. The PD generates photocurrent which goes to a transimpedance amplifier (TIA) on the carrier via CPW lines, as shown in Figure 2. The TIA has a bandwidth of 10 GHz, and converts the photocurrent from the 10 Gbps label into a voltage signal in order to drive external electronics, such as clock and data recovery circuits.

3. Label Recovery Experimental Results

First the PD on the integrated InP optical device was tested for label recovery by transmitting 128 bit, 10 Gbps NRZ optical labels (0101010101...01011) with 190 ns guard bands. The label was generated by entering a predefined pattern into a pattern generator which was linked to a bit error rate tester (BERT). The label pattern chosen has a sequence of 1s and 0s that is at the beginning of all labels used in our system. This sequence is needed for the clock and data recovery circuit intended to follow the label recovery. The RF output of the device was sent to an oscilloscope or BERT. For the measurements performed, the TWPD had no bias and the SOA can have current applied or can be unbiased to allow for simplified testing. Since the TWPD has shallow quantum wells and the SOA uses offset quantum wells, most of the light in the waveguide is not absorbed by an unbiased SOA and still reaches the PD in this scenario. A typical output from the device is shown in Figure 3a, showing that the detector does not saturate in burst mode. The entire label is shown in the center with close ups shown at the beginning and end. The BER measurements on the recovered labels are shown in Figure 3b. Label recovery can be performed error free for 0 dBm optical input power. Note, the BER measurement of the label recovery was performed directly with the output from the PD without any electrical amplifiers in between. With appropriate electrical amplifiers such as a burst mode amplifier, the sensitivity could be greatly increased.

In our experiments, the TIA used was not specifically designed for burst mode operation. We found that the amplifier decreased the extinction ratio of the label depending on the packet length and guard band due to the time constants of internal decision threshold circuits. In the future we will use an amplifier that is more linear and less susceptible to saturation.

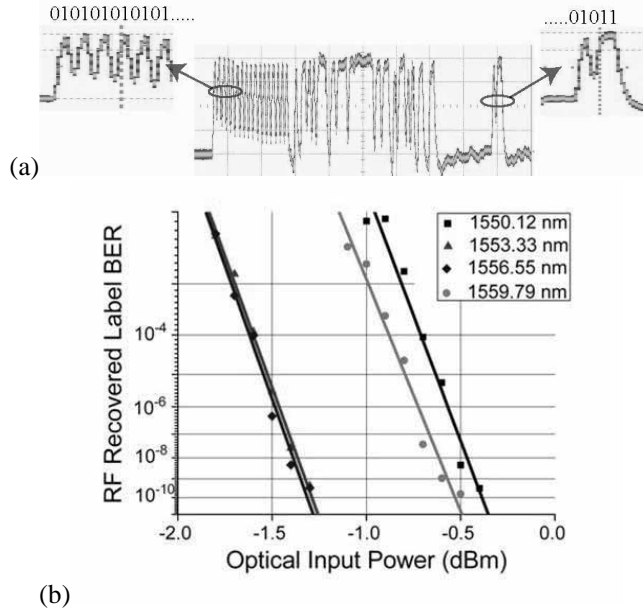


Fig. 3. (a) Recovered label output from the photodetector on InP. (b) Bit error rates for labels at four different wavelengths recovered by the photodetector on the integrated device. Optical input power refers to power into the integrated device (TWPd, SOA, and then PD).

4. Payload Envelope Detector Experimental Results

In non-packet mode operation the injection locked loop based clock recovery loop would be biased to run above the oscillation threshold to obtain a high quality recovered clock. However, an unsynchronized free-running signal occurs in the guard bands between the payloads [5]. In order to detect the payload envelope, we intentionally reduce the MMIC amplifier's gain so that the loop operates at around oscillation threshold, shown as the dashed curve in Figure 4. After 40 Gbps payloads were applied, shown in the top waveform in Figure 4 inset, the 40 GHz clock was recovered, shown as the solid curve in Figure 4. Its corresponding oscilloscope trace is shown in the lower waveform in Figure 4 inset. The recovered clock corresponds to the payload and the zero level corresponds to the guard bands.

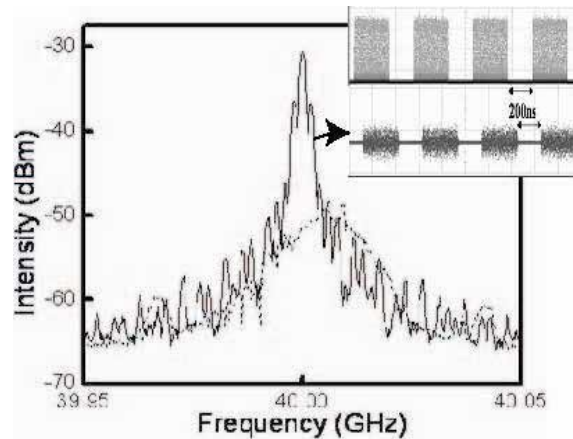


Fig. 4. RF spectra of the loop's free running signal at around oscillation threshold (dashed line) and injection locked recovered optical clock (solid line). (inset) Transmitted optical packets at 40 Gbps (upper) and electrical recovered 40 GHz packet clock (lower).

To obtain a PED signal, this packet clock signal is passed through an off chip Schottky envelope detector, which rectifies and self mixes the signal, resulting in the electrical signal shown in Figure 5a. The high level of the PED signal corresponds to the payload and the zero level corresponds to the guard bands. Note that this Schottky envelope detector could be integrated as component bonded to the carrier CPW line in the future using a commercially available surface mount product. This would avoid using any external components. This option was avoided at present to allow the device to be tested and used for 40 Gbps clock recovery as well. The 90/10 rise time of the PED signal was directly measured from the oscilloscope. The histogram mode of the oscilloscope was used to evaluate the RMS jitter of the PED signal. We found the PED signal has 3 ns rise and fall times and its RMS jitter is 150 ps limited by the oscilloscope. However, the jitter of the PED signal is estimated lower than 1ps considering the recovered 40GHz electrical clock has 643fs RMS jitter measured by an RF spectrum analyzer. The PED signal was demonstrated for variable length payloads from 8 ns long to 32 ns long as shown in Figure 5b.

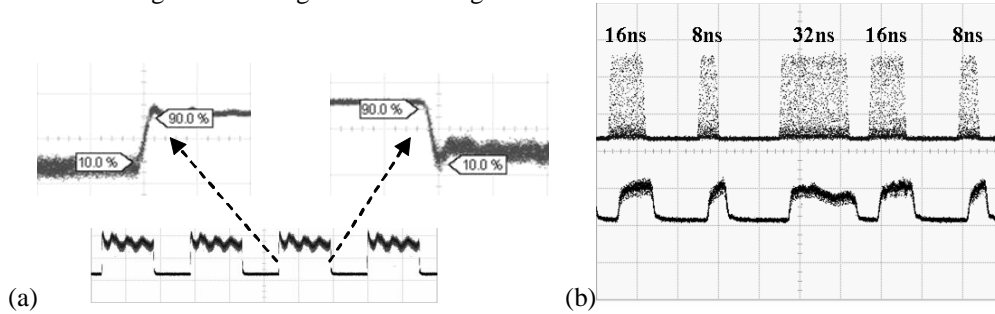


Fig. 5. (a) Electrical recovered PED signal showing the rise and fall of the signal. (b) Variable length optical packet input (top) and corresponding PED electrical signals (bottom).

5. Label Erasure and Rewriting using Payload Envelope Detection

To test the capability of our payload envelope signal, we used it in an experiment to erase labels and we then added new labels using a label rewriter. The experimental setup was similar to that shown in Figure 1 except the recovered label was not used for label lookup. Instead a predefined new label was inserted, and there was no wavelength conversion. To erase the label, we used the electrical PED signal to turn on an eraser SOA only during the high level of the PED signal. The eraser SOA was on a circuit board containing electronics that converted the PED voltage signal to a current signal large enough to turn the eraser SOA on and off. The optical data was split before entering the PED/OLR chip, and the part not sent to the chip was sent through a fixed optical delay before entering the eraser SOA. Since the rise time of the PED signal is consistent, a fixed optical delay means the electrical PED signal always arrived at the eraser SOA at the same time as the optical payload. Also, since the rise and fall time of the PED signal are the same, the PED signal duration is exactly matched to that of the payload, and the PED signal will not cut off any part of the payload. Thus the label was erased, while the payload was allowed to pass through the eraser SOA. Next a new label was added in the position of the old label using a laser and modulator to generate the new label. Figure 6 shows oscilloscope traces of the signal before entering the system, after label erasure, and after label rewriting. Bit error rates for the original label and the new label at 10 Gbps were performed and are also shown in Figure 6.

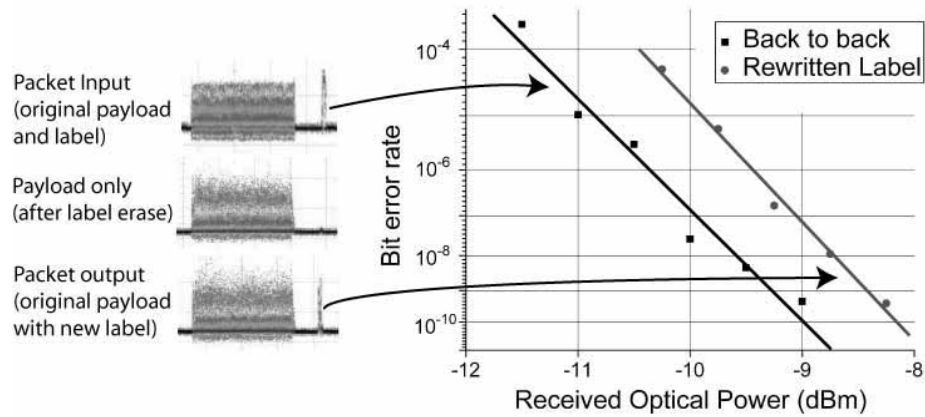


Fig. 6. Oscilloscope traces of the packet input, after label erasure, and after label rewrite. Also shown are the BERs for the original (back to back) and rewritten label.

The experiment described above is a simplification of an actual network node, but the results indicate that device can work well in a real system. As shown in Figure 1, after a packet enters the device the recovered label (which is recovered instantly) must be sent to a routing table where a new label/wavelength must be determined. That signal must then be sent to the label rewriter and wavelength converter. This process will take considerably longer than the 3 ns rise time of the PED signal. Thus the rise time will not affect system latency.

6. Conclusion

A hybrid integrated device has been designed and tested to perform optical payload envelope detection at 40 Gbps and optical label recovery at 10 Gbps. The device combines integrated InP optoelectronic devices with GaAs and InP electronics on a single carrier. The PED signal has a measured rise and fall time of 3 ns and RMS jitter of 150 ps. Error free optical label recovery and error free label erasure and insertion were demonstrated. The fabrication and integration techniques used to make this device indicate the potential for fully integrated optical label swapping.

This work is supported by LASOR award #W911NF-04-9-0001 under the DARPA/MTO DoD-N program.